Developmental and physiological responses of Brachypodium distachyon to fluctuating nitrogen availability

L. C. David, Thomas Girin, Eloïse Fleurisson, Elodie Phommabouth, Atem Mahfoudhi, Sylvie Citerne, Patrick Berquin, Francoise Daniel-Vedele, Annemarie Krapp, S. Ferrario-Mery

HAL Id: hal-02618607
https://hal.inrae.fr/hal-02618607

Submitted on 25 May 2020

SCIENTIFIC REP🞀RTS

Developmental and physiological responses of *Brachypodium distachyon* to fluctuating nitrogen availability

L. C. David, T. Girin , E. Fleurisson, E. Phommabouth, A. Mahfoudhi, S. Citerne, P. Berquin, F. Daniel-Vedele, A. Krapp & S. Ferrario-Méry

The Nitrogen Use Efficiency (NUE) of grain cereals depends on nitrate (NO_3^-) uptake from the soil, translocation to the aerial parts, nitrogen (N) assimilation and remobilization to the grains. *Brachypodium distachyon* has been proposed as a model species to identify the molecular players and mechanisms that affects these processes, for the improvement of temperate C3 cereals. We report on the developmental, physiological and grain-characteristic responses of the Bd21-3 accession of Brachypodium to variations in NO_3^- availability. As previously described in wheat and barley, we show that vegetative growth, shoot/root ratio, tiller formation, spike development, tissue NO_3^- and N contents, grain number per plant, grain yield and grain N content are sensitive to pre- and/or post-anthesis NO_3^- supply. We subsequently described constitutive and NO_3^--inducible components of both High and Low Affinity Transport Systems (HATS and LATS) for root NO_3^- uptake, and *BdNRT2/3* candidate genes potentially involved in the HATS. Taken together, our data validate Brachypodium Bd21-3 as a model to decipher cereal N nutrition. Apparent specificities such as high grain N content, strong post-anthesis NO_3^- uptake and efficient constitutive HATS, further identify Brachypodium as a direct source of knowledge for crop improvement.

The Poaceae family includes cereal crops such as wheat, rice, maize and barley, which provides a major source of food for humans and cattle. It is predicted that by 2050, the human population will increase by 20–50% in parallel to an increase of the living standard and thus, a doubling of grain demand is expected[1–3]. As arable land becomes limited, crop grain yields need to be improved. Nitrogen (N) is a major limiting macronutrient in the fields for crop production and as a consequence, N fertilizers are largely applied in modern agriculture to enhance plant vegetative growth and grain production. From an ecological point of view, the use of large amounts of N fertilizer on fields results in nitrate (NO_3^-) leaching, which causes eutrophication and biodiversity depletion. Thus, increasing crop yields while diminishing environmental impacts of agriculture is a major goal of today's agriculture. However, high-yielding modern cultivars are not suitable, as they have high nutrient requirements, due to their breeding under high nutrient availability[4,5]. Fundamental knowledge on molecular mechanisms of plant nutrition must be increased to engineer new cultivars giving high yields under low nutrient availability.

Mechanisms directly affecting the plant Nitrogen Use Efficiency (NUE) have been largely described at the physiological level in crop species (including wheat, barley, rice and corn) and in the model species, *Arabidopsis thaliana* (Arabidopsis)[6–9]. Most characterizations at the molecular level have however been restricted to the dicot Arabidopsis[10–12]. *Brachypodium distachyon* (Brachypodium) has been proposed as a good model to enhance this knowledge in C3 temperate cereals[13]. This non-domesticated monocot species offers convenient characteristics for academic research (simple diploid sequenced genome, short life cycle, simple growth requirement, large mutant collections, efficient genetic transformation), and is phylogenetically closely related to wheat and barley, enabling an efficient translational approach.

For grain crops, NUE is defined as the ratio between grain yield and available N in the soil per unit of field surface, and is often approximated as the ratio between yield and added N[14]. It is dependent on processes such as

Institut Jean-Pierre Bourgin, INRA, AgroParisTech, CNRS, Université Paris-Saclay, 78000, Versailles, France. L. C. David and T. Girin contributed equally. Correspondence and requests for materials should be addressed to T.G. (email: thomas.girin@inra.fr)

N uptake, translocation, assimilation and remobilization[11]. N is mainly taken up from the soil as nitrate (NO_3^-) and ammonium (NH_4^+) ions, thanks to specialized root transporters. NO_3^- being the most abundant form in aerobic fields, it constitutes the main N source for most temperate crops[11,15–17]. NO_3^- uptake relies on the activity of root High and Low Affinity Transport Systems (HATS and LATS, respectively), involving NO_3^- transporters of the NRT2 and NPF families[18–23]. HATS is active in low nitrate conditions (<1 mM) while LATS is predominant in higher nitrate concentrations. In many species, it has been shown that HATS is partly inducible by nitrate supply subsequently to nitrate deprivation (iHATS). In addition, a constitutive HATS is active under all environmental conditions (cHATS). The induction of HATS by NO_3^- is transient, and long exposure to NO_3^- and/or to other sources of N triggers a repression of NO_3^- influx[24–27]. Furthermore, HATS is a multi-component system since the interaction between NRT2 and its partner protein NRT3 is required for a functional NO_3^- transport activity[28]. In Brachypodium, 5 BdNRT2 genes have initially been identified by phylogenetic analysis and 2 more have been found in a subsequent analysis[13,29].

After being taken up from the soil, NH_4^+ is mainly assimilated in roots, while NO_3^- is mostly translocated to aerial organs, where it is successively assimilated into nitrite, NH_4^+, glutamine and glutamate by the consecutive actions of Nitrate Reductase (NR), Nitrite reductase (NiR) and the GS/GOGAT (Glutamine Synthetase/Glutamate Synthase) cycle[11,30]. Glutamate constitute the precursor of other amino acids and N-containing organic molecules of the plant[11,30]. During plant aging, remobilization processes take place, reallocating N from the source to sink organs[12]. In annual plants, the ultimate remobilization process is the monocarpic senescence (senescence of all vegetative organs), leading to plant death, while grains are filled with reserves[12]. The final NUE can potentially be improved by adjusting these physiological processes.

The potential of enhancing NO_3^- uptake/assimilation or N remobilization for increased grain yield is currently a matter of debate. Studies performed in rice, wheat and maize showed that more than half of the Grain Nitrogen Content (GNC) originate from leaf remobilization, and that this proportion depends on genotypes and soil N availability[31–33]. The importance of remobilization is also highlighted by an increased productivity of stay-green lines, having a delayed senescence[34]. Usually, this yield increase is however associated with a decrease in Grain Protein Content (GPC, directly related to grain N content), which is detrimental to the nutritional and food-processing qualities of the grain. Functional studies of wheat and barley NAM-B1 transcription factors suggest that, in some conditions, a tight control of senescence processes can lead to a higher GPC without decrease in grain yield[35,36]. On the other hand, it has been suggested that enhancing the post-anthesis N uptake is the main way to increase both yield and GPC in wheat[37,38].

To our knowledge, three studies have been published on N-related mechanisms in Brachypodium. Ingram and colleagues[39] analyzed the effects of N availability on root architecture and highlighted the variability of the response between accessions. Poiré and colleagues[40] revealed the stimulation of Brachypodium growth, leaf N content and photosynthetic capacity by high N availability during the vegetative stages. Hong and colleagues[41] showed that the interaction with symbiotic arbuscular mycorrhiza stimulates the expression of putative NH_4^+ transporters, but no effect was seen on N leaf content. As far as we know, no reported study in Brachypodium investigated the dependency of grain yield or GPC on physiological mechanisms such as N uptake, assimilation or remobilization.

Here, we report on a general characterization of Brachypodium physiology and responses to N availability, with a specific focus on grain production. We focussed on the Bd21-3 accession, as it is now the reference accession around the world due to its high transformation efficiency and to the availability of mutants in this background, allowing reverse-genetic approaches. We characterized the effects of NO_3^- availability at both vegetative and reproductive stages on growth, architecture, tissue composition and grain characteristics. We subsequently highlighted the unusual importance of post-anthesis NO_3^- uptake for grain N loading. Finally, NO_3^- transport systems were described at the physiological level, and candidate genes for root high affinity NO_3^- uptake were identified. This data provides a basis for molecular deciphering of NUE-related mechanisms in Brachypodium, as a model for temperate C3 cereals.

Results and Discussion

NO_3^- availability at vegetative stage impacts plant growth, development and tissue composition.

The effect of external NO_3^- availability on vegetative growth and development was investigated in 35-days-old plants, grown on sand and watered with a nutritive solution containing 0.1, 2 or 10 mM NO_3^- as sole source of N. The total fresh weight of plants grown on 0.1 mM NO_3^- was reduced when compared to the other conditions (64% reduction as compared to 10 mM NO_3^-). No significant difference was observed between plants grown on 2 and 10 mM NO_3^- (Fig. 1a; Supplementary Information Fig. S1). A similar effect was observed on the root fresh weight. In contrast, a reduction of shoot fresh weight (Fig. 1a) was already observed on 2 mM NO_3^- as compared to 10 mM NO_3^-, and more severe on 0.1 mM NO_3^-. Brachypodium Bd21-3 shoot biomass was thus more sensitive to NO_3^- limitation than root biomass, corresponding to the well documented decrease of shoot/root ratio under N limiting conditions (Supplementary Information Fig. S1b) in a variety of plants[42,43], and to a previous study on Brachypodium Bd21-3[40].

Tillering is a primordial characteristic of cereals, as it influences the number of spikes and thus the grain yield. To further characterize the effect of N availability, the main stem and the different tillers (Fig. 1b) were separated. At 0.1 mM NO_3^-, only 40% of the plants developed a first tiller (data not shown) and none developed tillers of higher ranks. In the other conditions, all plants produced 3 tillers, in addition to the main stem. This effect of N availability on tiller number is consistent with observations made in wheat and barley[44–46]. As for total shoot, the fresh weight of the main stem and of tillers of different ranks were progressively reduced with the reduction of NO_3^- availability (Fig. 1c). Thus, both shoot growth and development were limited by low N availability on 0.1 mM NO_3^-, whereas only shoot growth was affected on 2 mM NO_3^-, with a similar effect on the main stem and tillers.
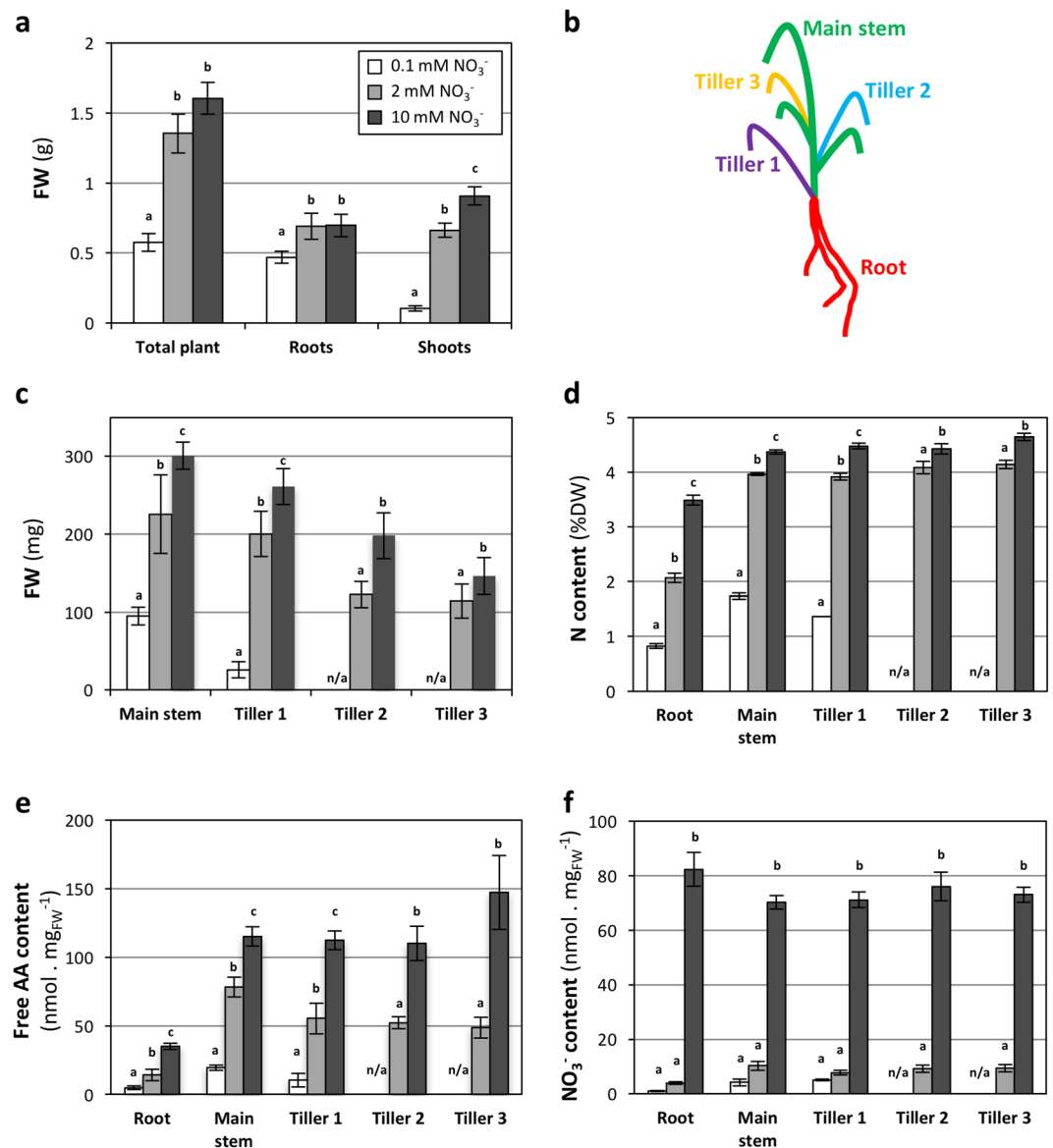
Figure 1. Effects of NO_3^- availability at vegetative stage. Plants were grown on sand for 35 days, watered with nutritive solution containing 0.1, 2 or 10 mM NO_3^-. **(a)** Fresh weight of total plant, roots and shoots. **(b)** Schematics of tiller development. Tiller were numbered according to their sequential apparition. **(c)** Fresh weight, **(d)** N content, **(e)** Free AA content and **(f)** NO_3^- content of main stem and tillers. Values correspond to the mean of 4 or 5 biological replicates (2 plants each) $+/-$ SD. Letters indicate statistical groups for each plant part (Non-parametric ANOVA, $p < 0.05$). N/a: no data available, due to the lack of development of tillers 2 and 3 in the 0.1 mM NO_3^- condition.

To characterize the effect of NO_3^- availability on the plant, Nitrogen (N), Carbon (C), free amino acids (AA) and NO_3^- contents of the tissues were measured. Nitrogen content was reduced in all parts of the plant (roots, main stem and tillers) on both 0.1 and 2 mM conditions as compared to 10 mM NO_3^-, with a stronger effect on 0.1 mM (Fig. 1d). The nitrate availability had a minor effect on C content (Supplementary Information Fig. S1c). Consequently, C/N ratio was reduced by increasing NO_3^- availability, with similar patterns for the different plant parts (Supplementary Information Fig. S1d). The effect on AA content was qualitatively similar to that observed on N content, with significant differences between the three conditions, and comparable effects on all parts of the plant (Fig. 1e). Free AA content was quantitatively more affected than N content at the whole plant level, with 91% and 55% global decrease on 0.1 mM and 2 mM, respectively, when compared to 10 mM (whole plant N content was reduced in parallel by 76% and 25%) (Supplementary Information Fig. S1e,f). Nitrate content was also strongly affected in all plant parts by low external NO_3^- availability (Fig. 1f), being globally reduced by 98% and 91% on 0.1 and 2 mM, respectively (Supplementary Information Fig. S1g).

Thus, external NO_3^- limitation led to a strong decrease of internal NO_3^- pools and a strong to moderate decrease of both free AA and N contents, leading to a moderate effect on plant growth and development.

Interestingly, the main stem and initiated tillers responded similarly to reduced NO_3^- availability, suggesting there is no prioritization for N allocation between main stem and tillers.

Both pre- and post-anthesis NO_3^- availability affect vegetative growth and grain yield. Based on the effects seen at the vegetative stage, we further investigated the effects of pre- and post-anthesis N availability on end of cycle plant and grain characteristics. Plants were grown hydroponically on a medium containing NO_3^- as a sole source of N. Control plants (Ctrl) were maintained on media containing $1\,mM\ NO_3^-$. This condition was chosen based on the previous experiment. This nitrate concentration should lead to intermediate growth and N physiological state of the plants, enabling to test both positive and negative effects of changes in external NO_3^- availability. Four treatment conditions were used: plants grown on media containing either low N (LN; $0.1\,mM\ NO_3^-$) or high N (HN; $10\,mM\ NO_3^-$) until anthesis of the first spikes, then transferred to $1\,mM\ NO_3^-$; and conversely, plants grown on $1\,mM\ NO_3^-$ until anthesis, then transferred to LN or HN. Plants grown in the three different conditions at vegetative stage sequentially reached the anthesis stage (Supplementary Information Fig. S2a). Plants grown at vegetative stages on 0.1 and $1\,mM\ NO_3^-$ exhibited similar fresh weights at anthesis, despite a shift to reach this stage, whereas plants grown on $10\,mM\ NO_3^-$ were more developed (Supplementary Information Fig. S2b).

At the end of the cycle, grain yield per plant was increased by pre-anthesis HN treatment (+68%), reduced by post-anthesis LN treatment (−42%), and not affected in other conditions (Fig. 2a). The shoot dry weight followed a similar pattern (+56%, −26% and no effect, respectively; Fig. 2b). Accordingly, the harvest index (grain/total above-ground dry weights) was not affected by the treatments as compared to the control condition (Supplementary Information Fig. S2c), suggesting that the variations in grain yield are a consequence of variations in vegetative growth. In barley and wheat, grain yield is similarly dependent on the vegetative biomass, which related to the nitrogen fertilization[44,47]. In contrast, the effect of post-anthesis N availability (LN treatment) on grain yield and shoot biomass was surprising, as it is usually not observed in cereals[37,48,49]. This was linked to the continuation of shoot growth after anthesis, whereas it is generally admitted that vegetative growth stops around anthesis stage in cereals[37]. The maintenance of vegetative growth after anthesis in Brachypodium Bd21-3 might be linked to the undomesticated nature of the species. In addition, it could have been enhanced by the growing conditions used in our study, as it has been reported that tillering hydroponic-grown wheat can continue for an indefinite time, under non-limiting conditions[44].

Plants grown on $10\,mM\ NO_3^-$ up to anthesis and subsequently on $1\,mM\ NO_3^-$ presented higher end-of-cycle shoot biomass and grain yield than the control plants. In contrast, shoot biomass and grain yield were not stimulated by the 10 mM post-anthesis treatment when compared to the control, and were reduced by the 0.1 mM post-anthesis treatment. Thus, in our conditions, $1\,mM\ NO_3^-$ was sufficient for maximal growth in late, but not in early development. This is consistent with the observation made by Gastal and Lemaire[50], that the N uptake demand from the plant to achieve maximal growth decreases as the plant gets bigger. Our observation might thus reflect the negative relationship between plant biomass and N supply necessary for maximum growth, known as the critical N curve and observed for many crops[50,51].

Grain yield depends on grain number and grain abortion rate. Grain yield in C3 temperate cereals is known to be affected by environmental conditions through both grain number and grain size[52–55]. Thus, we explored the effects of N availability on these traits. The grain number per plant was increased by pre-anthesis HN treatment and reduced by post-anthesis LN treatment (+65% and −40%, respectively; Fig. 2c), whereas the individual grain weight was not affected (Fig. 2d). This established a direct link between grain yield and grain number. Such an absence of an effect of N nutrition on grain weight has previously been described for wheat grown in pots or in hydroponics[44,56]. It is thus possible that grain weight is more sensitive to N availability in the field than in controlled conditions.

We subsequently analyzed the basis of the variation of grain number. The pre-anthesis HN treatment did not statistically increase the number of spikes (equal to the number of tillers, as all tillers developed spikes in the 5 conditions), nor the grain number per spike (Fig. 2e,f). This suggests that the increased grain yield in this condition is due to slight multiplicative increases in both the number of tillers and the grain number per spike. On the other hand, the yield decrease in the post-anthesis LN treatment correlated with a strong reduction of spike number (−82%; Fig. 2e) and a high increase in average grain number per spike (+261%; Fig. 2f). This increase in grain number per spike was due to a reduction of grain abortion to 25% of grain initiation, as compared to 53% in the control condition (Supplementary Information Fig. S2d). Thus, the post-anthesis initiation of tillers was restricted by low N availability, but grain production was partially compensated by a greater development of the spikes. Interestingly, the general high proportion of grain abortion confirms the observation by Oscarson[44], stating that in most N conditions, wheat plants produce slightly more tillers than can be supported for grain filling. The author hypothesized that producing extra tillers enables the plant to produce more grains in case of a late increase in nutrient availability.

Post-anthesis N availability affects N and protein contents and free AA composition of the grains. We investigated the effect of the pre- and post-anthesis N treatments on grain composition, including N and protein contents. Grain protein content (GPC), directly related to grain N content (GNC), is a main criterion for cereal grain quality, in relation to the end-use. For malting barley, the GPC should be in the range of 8.5–12.5% DW (corresponding to GNC of 1.4–2% DW), and can be higher for feed barley[57,58]. A high protein content is favorable for the baking quality of wheat flour[59], and GPC between 10–15% are thus usually reported for bread wheat grains (corresponding to GNC of 1.75–2.6%)[8,37,60,61]. Recently, high GNC (ranging 2.3–3.0%) has been reported in bread wheat grown in a semi-hydroponic system[49]. In our experiment, GNC was around 3% DW (Fig. 3a), corresponding to an estimated GPC of 17% DW when using the accepted conversion factor of
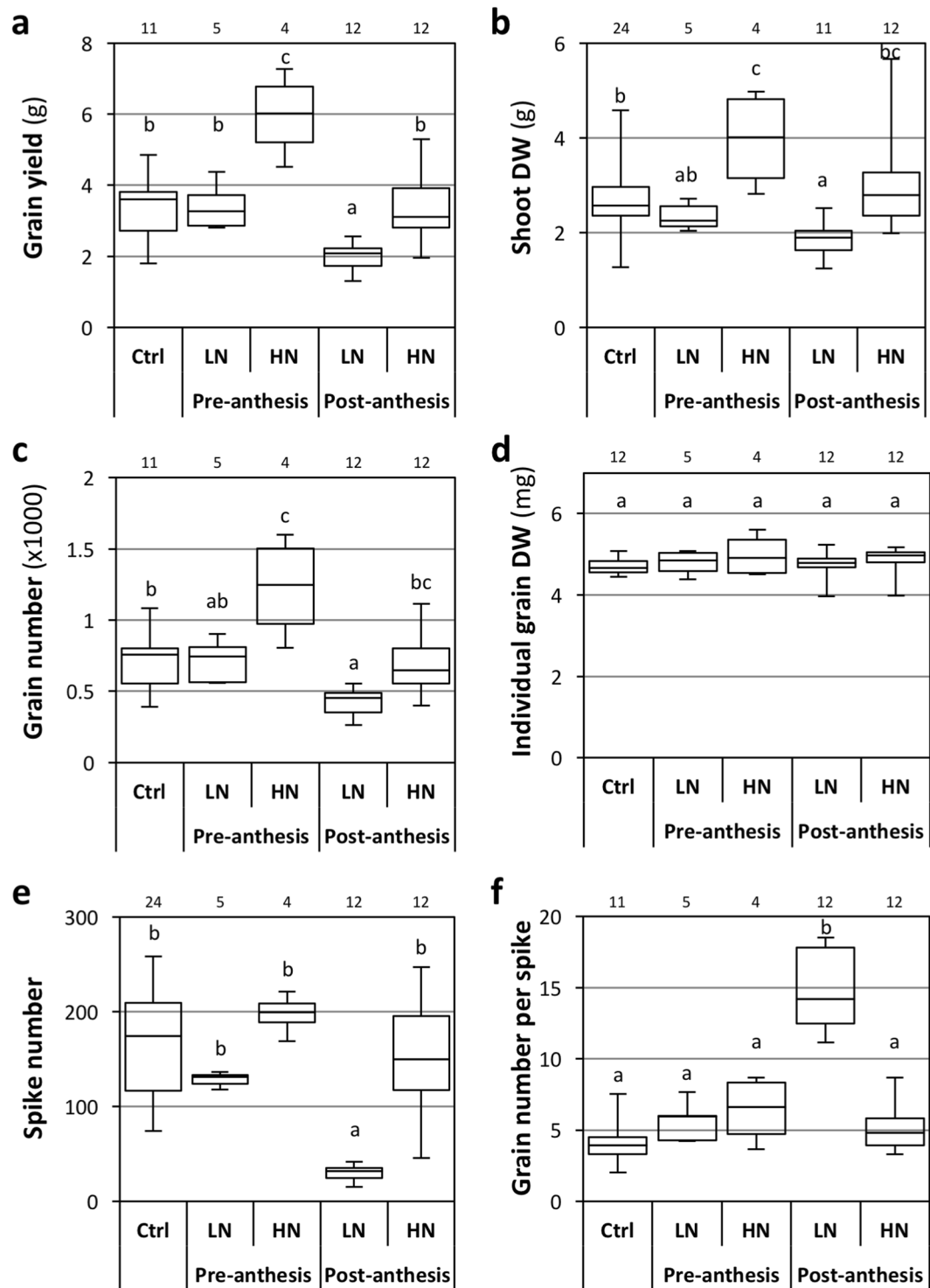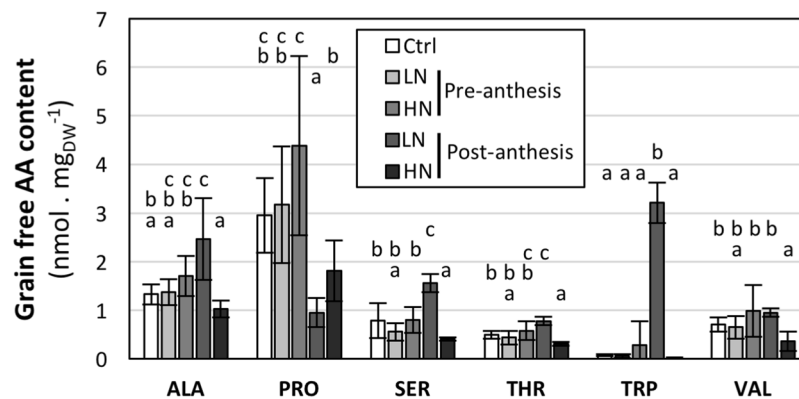
Figure 2. Effects of pre- and post-anthesis NO_3^- availability on end of cycle characteristics. Plants were grown in hydroponics. Ctrl: control plants grown on 1 mM NO_3^- during the entire life cycle. Pre-anthesis: plant grown on 0.1 or 10 mM NO_3^- (LN and HN, respectively) until anthesis, and subsequently on 1 mM NO_3^-. Post-anthesis: plant grown on 1 mM NO_3^- until anthesis, and subsequently on LN or HN. (**a**) Grain yield per plant. (**b**) Shoot Dry Weight (DW). (**c**) Grain number per plant. (**d**) DW of individual grain. (**e**) Spike number per plant. (**f**) Grain number per spike. The boxplots represent minimum, 1st quartile, median, 3rd quartile and maximum values. Letters indicate statistical groups (Non-parametric ANOVA, p < 0.05). Number of biological replicates for each condition are indicated above the charts.
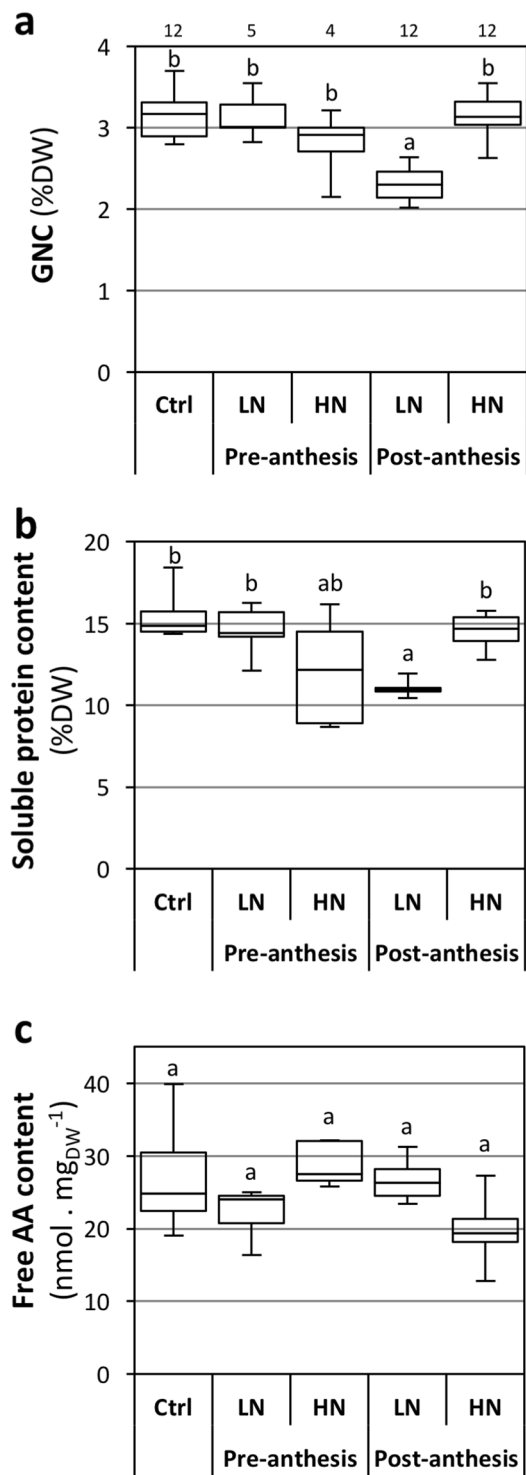
Figure 3. Effects of pre- and post-anthesis NO_3^- availability on grain composition. Growing conditions and treatments were as described in Fig. 2. LN, Ctrl and HN: 0.1, 1 and 10 mM NO_3^-, respectively. Grain contents in (**a**) total N (GNC), (**b**) extractable proteins and (**c**) free AA. The boxplots represent minimum, 1st quartile, median, 3rd quartile and maximum values. Letters indicate statistical groups (Non-parametric ANOVA, $p < 0.05$). Number of biological replicates for N content are indicated above the chart; other charts are based on 5 biological replicates per condition.

5.7[62]. Our results are in agreement with the high GNC (2.9–3.7%) reported for Brachypodium Bd21-3 in different growth conditions[63,64]. These results underline the generally high grain N content of Brachypodium Bd21-3, and identify this species (or at least this accession) as a source of knowledge for the improvement of bread wheat GPC.

Figure 4. Effects of pre- and post-anthesis NO_3^- availability on grain free AA composition. Growing conditions and treatments were as described in Fig. 2. LN, Ctrl and HN: 0.1, 1 and 10 mM NO_3^-, respectively. Only free AA levels affected by the treatments are presented; see Table S1 (Supplementary Information) for full set of data. Values are means of 5 biological replicates +/−SD. Letters indicate statistical groups for each AA (Non-parametric ANOVA, p < 0.05).

The GNC was quite unaltered by pre- and post-anthesis N treatments (Fig. 3a), as it was statistically affected only by the post-anthesis LN treatment (−27%). In combination with the reduction of grain yield in this condition, this highlights the sensitivity of Bd21-3 to low N availability for grain quality and quantity during the reproductive phase. Interestingly, GNC was unaffected by the pre-anthesis HN treatment that triggered an enhanced grain yield, underlining independency between the traits. Cereal GNC is known to be highly dependent on post-anthesis N uptake and on remobilization from vegetative organs of N assimilated before anthesis[37,48,65]. Accordingly, a late field application of fertilizer is usually recommended to improve grain N uptake during grain filling, and thus grain protein content[66], as observed in our experiment. The source limitation of GNC was apparent for low N treatment, showing that N remobilization could not compensate the reduction of external N availability. This is in agreement with the dominance of post-anthesis uptake over remobilization for grain N filling in our conditions (see thereafter).

Compared to the control condition, the grain C content was marginally reduced under all treatments, except by the pre-anthesis LN treatment (Supplementary Information Fig. S2e). The C/N ratio was only significantly modified in the post-anthesis LN treatment (Supplementary Information Fig. S2f). The grain content in soluble proteins followed the same pattern as the GNC, with only the post-anthesis LN condition presenting a significant difference with the control (−26%; Fig. 3b). The grain soluble protein content ranged between 10–15%, which is consistent with published studies in Brachypodium Bd21-3[63,64]. The grain composition in soluble protein was visualized by SDS PAGE (Supplementary information Fig. S3). The protein profile was consistent with a previous report on Brachypodium grain protein composition[63], and no major differences in the protein profiles was found between the treatments.

Although grain free amino acid (AA) content represents a small proportion of total grain N content (less than 1%)[67] when compared to seed protein (around 60%), it could indicate an effect of N availability on grain N storage capacity[68]. The free AA pool results from the balance between neo-synthesis in grain and AA remobilization from leaves on the one hand, and seed protein synthesis during grain development on the other. In our experiment, no significant change in total free AA content was observed (Fig. 3c), suggesting an absence of global nitrogen imbalance between grain AA supply and seed protein synthesis. In contrast, the analysis of the free AA composition revealed some specific changes. For instance, Asn (27–44% of free AA), Pro (4–17%), Gln (5–10%), Ala (5–10%), Asp (5–7%), Ser (3–6%), Glu (3–6%) and Arg (3–6%) represented the main free AA's in the grain (Supplementary Information Table S1). Post-anthesis treatments induced significant changes in the content of some of the free AA's (Fig. 4). Post-anthesis LN treatment triggered a large increase in Trp (x45), moderate increases in Thr, Ser, and Ala, and a decrease in Pro (x1/3) (Fig. 4). Post-anthesis HN treatment triggered moderate decreases (x1/2) in Thr, Ser and Val. The effects of post-anthesis treatments on the free AA pool may result from specific variations in N remobilization or protein synthesis.

The storage proteins in Brachypodium Bd21-3 grains are composed mainly of globulins (50–60%) and prolamins (12%), similar to that in rice and oat[64]. The major AA's of grain proteins are Glx, Asx, Pro and Gly (20%, 10%, 8.6% and 8.5% respectively)[64]. In wheat, accumulation of prolamins correlates with the post-anthesis N supply[65,69]. Interestingly, Brachypodium prolamins are homologous to wheat avenin-like and γ-gliadins, the latter being characterized by a high content in Pro (17.4%)[64]. Thus, the decrease of grain free Pro content in our post-anthesis LN treatment could correlate with a limitation in prolamin synthesis. Additionally, the lower protein level observed in post-anthesis LN suggests that N fertilization has the same effect on prolamin as it does in wheat. The other major free AAs (Glx, Asx, and Gly) found in grain proteins of Brachypodium Bd21-3 did not show significant changes in the free AA pool. Some less abundant amino acids (Thr, Ser, Ala, and Val) were increased by post-anthesis N limitation and/or decreased by post-anthesis N abundance, thus were likely not limiting for globulin synthesis. Trp is an essential amino acid for human and animal nutrition and is usually in limiting concentrations in wheat grain. We observed a spectacular increase of Trp in the grains after post-anthesis LN

treatment. Trp was below the detection threshold in a previous study[64], due to the methodology (acidic hydrolysis of protein) that degrades this AA. Trp content in prolamin varies between grain cereals, being lower in wheat prolamin than in the globulin fraction[67,70]. Thus, our results highlight a limitation in seed protein synthesis, probably in prolamin but also in globulin after post-anthesis LN treatment.

Grain N loading depends primarily on post-anthesis N uptake.

Our data highlighted an important correlation of both grain quality and quantity with post-anthesis NO_3^- availability (Figs 2 and 3), thus we further characterized N fluxes in the plant at this stage. N grain loading in cereals is dependent on both N remobilization from vegetative organs (taken up before anthesis) and post-anthesis N uptake[37,48,65]. We thus quantified both processes and investigated their coordinated responses to variations in NO_3^- availability. Plants were grown hydroponically on media containing 0.2 mM NO_3^- until anthesis of the first spikes, then transferred to conditions of either N deprivation, limitation or abundance (0.01 (A), 0.2 (B) and 10 (C) mM NO_3^-, respectively). These contrasting conditions were chosen to maximize the effect of the treatments on both grain yield per plant and GNC (Supplementary Information Fig. S4). A pulse-chase strategy was used at the vegetative phase (replacement of the NO_3^- by $^{15}NO_3^-$ for 5 days) to enrich the vegetative tissues with ^{15}N stable isotope. Plants were harvested either at anthesis (to map the ^{15}N distribution at the end of vegetative phase) or after full senescence of the plant. Roots, shoots and spikes were collected separately, and dry weight, N content and ^{15}N enrichment were measured (Supplementary Information Table S2). Nitrogen fluxes between plant parts after anthesis were then calculated as previously described[71].

The post-anthesis NO_3^- uptake was stronger than remobilization fluxes from vegetative shoots and roots in all conditions, and was highly stimulated by NO_3^- availability (Fig. 5; see Supplementary Information Table S3 for statistical tests). Hence, end of cycle grain N originated mainly from NO_3^- taken up at the post-anthesis stage (59% to 91%, in deprivation and abundance conditions, respectively). Grain N originating from remobilization was significantly reduced under high N availability, both on relative values (9% and 41% of grain N under abundance and deprivation, respectively) and on absolute quantities (4.8 and 6.5 mg$_N$), reflecting a negative effect of N availability on N remobilization. The proportion of total plant N localized in the grain at the end of the cycle was relatively high in all conditions, ranging from 65% under abundance to 73% under deprivation (Fig. 5). This was consistent with the strong allocation of post-anthesis N uptake to the grain (65% to 70%).

In cereals such as wheat, barley, rice and maize, remobilization is regarded as the main N source for grain loading, providing 60–90% of the final grain N, depending on genotypes and environmental conditions[32,33,48,56,72]. In our experiment, remobilization had a minor role, furnishing 9–41% of grain N depending on post-anthesis NO_3^- availability. A low importance of remobilization has recently been described in wheat: out of 8 measurements (2 genotypes grown in 4 conditions, including low and high N availability), 7 ranged from 0% to 37%, and only one had a value above 50%[49]. This study, based on plants grown in a semi-hydroponic system in a growth chamber, could suggest that our observed low values are linked to our experimental setup. Alternatively, it has been reported that a low pre-anthesis and/or a high post-anthesis N availability reduce the contribution of remobilization for grain loading[49,73,74], which may be the case in our study. Finally, it is also possible that grain N loading in Brachypodium Bd21-3 is mainly based on post-anthesis N uptake, rather than on N remobilization. A similar case has been reported for instance in sorghum[75,76] and in stay-green maize genotypes[77]. In the case of Brachypodium, the relative importance of post-anthesis NO_3^- uptake could be related to the non-domesticated nature of the species. Investigating several Brachypodium accessions, each grown in various conditions, would be necessary to confirm whether a genetic and/or environmental effect is the reason for this high contribution of post-anthesis NO_3^- uptake for grain N loading.

High external NO_3^- availability had a strong positive effect on NO_3^- uptake and a weak, but significant, repressive effect on N remobilization from shoots to grains (6.2 mg$_N$ on 0.2 mM NO_3^- *versus* 4.8 mg$_N$ on 10 mM NO_3^-). This reduced remobilization in situations of high post-anthesis N uptake have frequently been observed in wheat[37,49,78–80]. As highlighted by Bancal[81], the difference in remobilization has a limited impact on the N distribution to the grain (1.4 mg$_N$ difference in remobilization between 0.2 and 10 mM conditions, to be compared to a total grain N content of 37.3 and 63.8 mg$_N$; Fig. 5). Accordingly, the NO_3^- availability had no statistically significant effect on N partitioning (73% of the total plant N was located in the grain on 0.01 mM NO_3^-, and 65% on 10 mM NO_3^-). The Nitrogen Harvest Index (NHI; proportion of above-ground N localized in the grains) was between 70% and 82% (on 10 mM and 0.01 mM NO_3^-, respectively), which is comparable to values observed in wheat, barley and oilseed rape[8,61,82], and much higher than in Arabidopsis (25–53%)[7].

NO_3^- uptake is mediated by constitutive and inducible HATS and LATS.

Due to the importance of NO_3^- uptake for grain N loading, we further investigated characteristics of NO_3^- influx. In most studied plants – such as barley, wheat, Arabidopsis and *Brassica napus* – root NO_3^- uptake is performed by three classes of systems: constitutive High Affinity Transport Systems (cHATS), inducible HATS (iHATS) and constitutive Low Affinity Transport System (cLATS)[26,83–87].

N-deprived plants grown hydroponically were either induced with 1 mM NO_3^- for 24 h or remained uninduced. Root NO_3^- influx was then measured at external concentrations ranging from 0 to 10 mM. Influx was enhanced by the NO_3^- pre-treatment for all the tested concentrations, highlighting the inducibility of the uptake capacity (Fig. 6a). The influx curves were composed of two phases, indicating the involvement of HATS and LATS. HATS was active at low NO_3^- concentration, reaching saturation at around 0.2 mM NO_3^- (Fig. 6b). Constitutive HATS (cHATS) was active in the absence of NO_3^- pre-treatment, whereas both cHATS and inducible HATS (iHATS) contributed to the activity of HATS after NO_3^- pre-treatment (Fig. 6b). Both cHATS and iHATS followed Michaelis-Menten kinetics, with similar Vmax and Km values (Fig. 6b,c). The induction by NO_3^- of HATS was relatively low (factor 2.5) compared to other studies, where induction factors of 5–30 are often reported[26]. Interestingly, cHATS Vmax was higher than what has been described in wheat and barley in similar
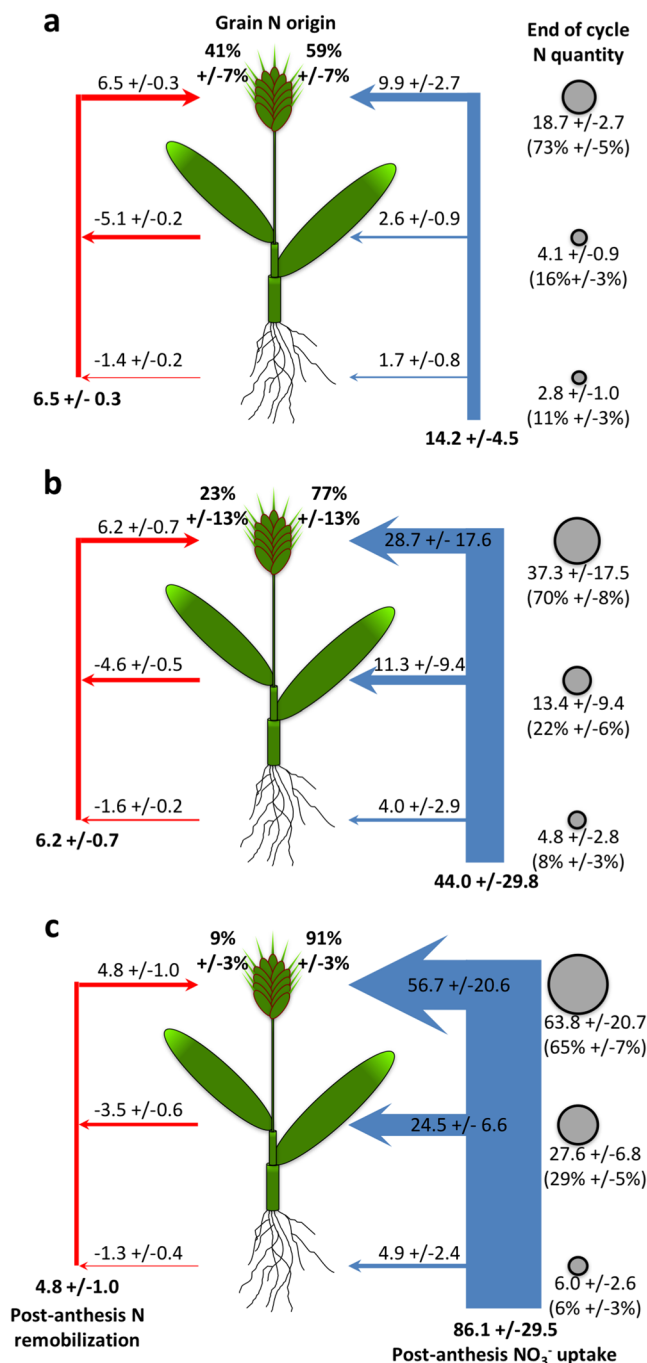
Figure 5. Effect of post-anthesis NO_3^- availability on N fluxes. Plants were grown hydroponically on 0.2 mM NO_3^- and transferred at anthesis to **(a)** 0.01, **(b)** 0.2 or **(c)** 10 mM NO_3^-. Left arrows (red): post-anthesis remobilization of pre-anthesis N pools from vegetative plant parts. Right arrows (blue): post-anthesis NO_3^- uptake. Arrows indicate the N fluxes from/to spikes, shoots or roots; values of the fluxes (mg_N) are specified above the arrows. Bold values at the bottom of the panels correspond to total N remobilization (left) and total NO_3^- uptake (right) at the plant level (mg_N). Percentages above the spikes indicate the proportion of grain N originating from remobilization (left) and from post-anthesis uptake (right). Total N quantities in spikes, shoots and roots after full senescence of the plants are indicated by circles on the right of each panel; absolute values (mg_N) are indicated; distribution of N quantity between spikes, shoots and roots are specified in brackets (% of the plant total N). Values correspond to the mean of 5 (panel a) or 7 (panels b and c) biological replicates $+/-$ SD. Raw data (DW, N content and ^{15}N enrichment of the different plant parts) and results of statistical tests are presented in Supplementary tables ST2 and ST3, respectively.

conditions (1.9 compared to 0.3–0.8 $\mu mol_N \cdot g_{FW}^{-1} \cdot h^{-1}$), whereas cHATS + iHATS Vmax corresponded to the low range seen in wheat and barley (4.8 compared to 4–12 $\mu mol_N \cdot g_{FW}^{-1} \cdot h^{-1}$)[26,83,88–90]. This suggests that the HATS is characterized by both a strong basal activity and a relatively weak inducibility by NO_3^- in Brachypodium Bd21-3.
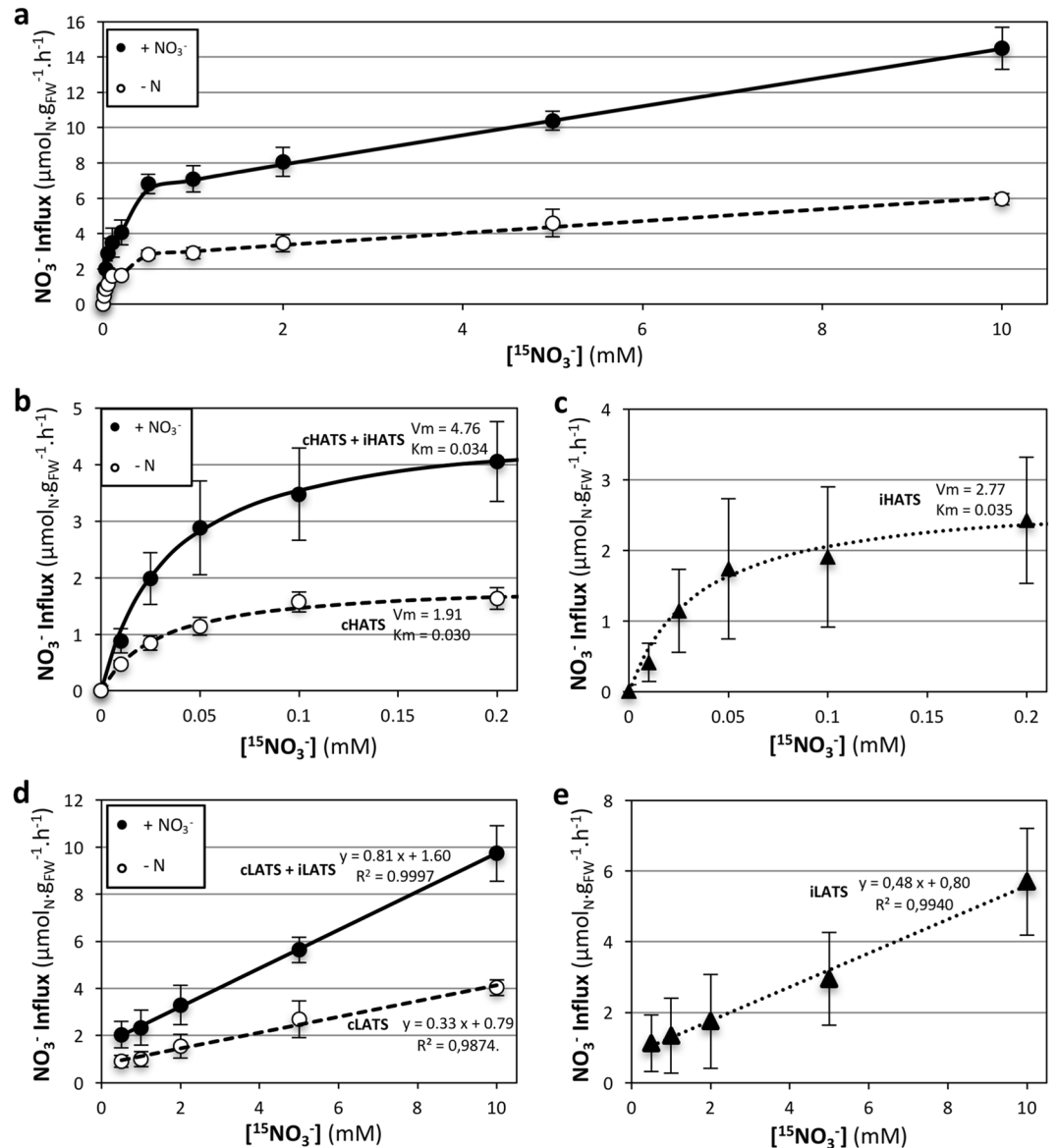
Figure 6. Characterization of High and Low NO_3^- Transport Systems (HATS and LATS, respectively). Plants were grown hydroponically on 2 mM NO_3^- for 7 days, then N starved for 8 days (−N, open circles and dashed lines) or N starved for 6 days and induced with 1 mM NO_3^- for 24 h (+NO_3^-, closed circles and solid lines). (**a**) $^{15}NO_3^-$ influx at external concentrations ranging from 0.01 to 10 mM $^{15}NO_3^-$. (**b**) $^{15}NO_3^-$ influx at external concentrations ranging from 0.01 to 0.2 mM $^{15}NO_3^-$. HATS kinetics were fitted with Michaelis-Menten curves ($Influx = Vmax * [^{15}NO_3^-]/(Km + [^{15}NO_3^-])$). Vmax and Km values were obtained by linear regression on the Lineweaver-Burk representation ($1/Influx = a * (1/[^{15}NO_3^-]) + b$, with $Vmax = 1/b$ and $Km = a/b$). cHATS and iHATS: constitutive and inducible HATS (respectively). (**c**) iHATS influx at external concentrations of 0.01–0.2 mM $^{15}NO_3^-$, obtained by subtracting −N values from +NO_3^- values in panel b and fitted with Michaelis-Menten curve. (**d**) LATS $^{15}NO_3^-$ influx at external concentrations ranging from 0.5 to 10 mM $^{15}NO_3^-$, obtained by subtracting HATS Vmax values (panel b) from corresponding influx values (panel a). LATS kinetics were fitted with linear curves. cLATS and iLATS: constitutive and inducible LATS (respectively). (**e**) iLATS curve, obtained by subtracting values from −N condition to values from +NO_3^- condition in panel d, fitted with a linear curve. Values correspond to the mean of 5 biological replicates +/−SD.

These characteristics might reveal an adaptation to N-poor natural habitats, in accordance with the origin of this accession from an arid region in Iraq, a typical ecosystem where N availability is low[91,92].

LATS activity was calculated by subtracting the Vmax values of the HATS from the corresponding measured influx in the range 0.5–10 mM NO_3^-. Surprisingly, the LATS activity was induced by NO_3^- pre-treatment (Fig. 6d). Both constitutive LATS (cLATS) and inducible LATS (iLATS) followed a linear curve in the studied range (Fig. 6d,e). This existence of iLATS has not been observed in most species including barley, in which extensive studies have been performed[26,83,84,93]. To our knowledge, an iLATS has only been unambiguously reported
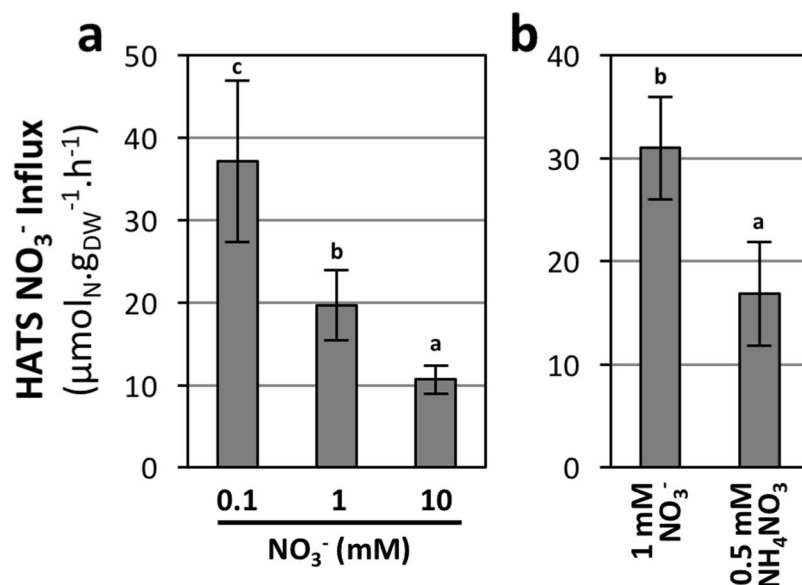
Figure 7. Responses of HATS to N availability. HATS was quantified at 0.2 mM $^{15}NO_3^-$ on 17-day-old plants grown hydroponically on either **(a)** 0.1, 1 or 10 mM NO_3^- or **(b)** 1 mM NO_3^- and transferred for 24 h to 1 mM NO_3^- or 0.5 mM NH_4NO_3. Values correspond to the mean of 5 biological replicates +/−SD. Letters indicate statistical groups (Non-parametric ANOVA, $p < 0.05$).

in wheat and in *Populus tremuloides*[94,95]. This highlights the suitability of Brachypodium Bd21-3 as a model for NO_3^- uptake systems in wheat.

HATS is regulated by N availability, likely involving *BdNRT2/3* genes.

High affinity NO_3^- transport systems are of prime importance for crop improvement, as ideal varieties should have a high uptake capacity at low NO_3^- availability. The regulations of HATS activity were further investigated by cultivating plants under contrasting conditions of steady state N availability or by treating them for 24 h with NH_4NO_3. HATS activity was then measured by transferring the plants for 5 minutes on 0.2 mM $^{15}NO_3^-$ nutrient solution. HATS influx was gradually reduced by increasing NO_3^- availability from 0.1 to 10 mM NO_3^- (Fig. 7a). Similarly, HATS activity was repressed by the presence of ammonium (NH_4^+) in the medium (Fig. 7b). This is consistent with the repression of HATS by increased levels of NO_3^- or by other sources of N, described in other species[24–27].

HATS has been described in several species as mediated by NRT2 transporters, in interaction with NRT3[28,96]. We previously identified seven *NRT2* and two *NRT3* genes in Brachypodium[13]. We investigated the expression of four co-orthologs (*BdNRT2A* to *BdNRT2D*) of the major *NRT2* genes identified in Arabidopsis and barley (*AtNRT2.1* and *HvNRT2.1*, respectively). Due to nearly identical coding sequences of *BdNRT2A* and *BdNRT2B* in Bd21-3 accession, these genes were quantified simultaneously. The quantification of gene expression was done by RT-qPCR in parallel to the characterization of HATS regulations (above), on independent plants. The investigated genes were more expressed in roots than in shoots (Fig. 8a). Whereas *BdNRT2C* and *BdNRT2D* expressions were insensitive to NO_3^- availability, *BdNRT2A/B* were repressed by high NO_3^- (Fig. 8a) and NH_4^+ (Fig. 8b), as observed for the HATS (Fig. 7). *BdNRT3* genes were also mainly expressed in the roots (Fig. 8c). Expression of *BdNRT3.1* was unchanged under all NO_3^- supplies, whereas *BdNRT3.2* was repressed by high NO_3^- concentrations (Fig. 8c). *BdNRT2A/B* and *BdNRT3.2* thus constitute good candidates to be involved in HATS activity in these conditions in Brachypodium Bd21-3, as they are mainly expressed in the roots, and their expression pattern follows the HATS activity.

The expression of *BdNRT2A/B* and *BdNRT3.2* was also investigated at post-anthesis stage in the experiment dedicated to the characterization of the effects of NO_3^- availability pre-anthesis and post-anthesis. *BdNRT2A/B* expression was stimulated by the pre-anthesis HN treatment (Fig. 9a). In this condition, the vegetative biomass production was enhanced before anthesis (see Fig. S2B), triggering a high post-anthesis N demand from the plant on 1 mM NO_3^- and thus explaining the stimulation of *BdNRT2A/B* expression. In the post-anthesis LN condition, the expression seemed also higher than in the control condition, despite being not statistically significant (Fig. 9a). In both situations, a high N demand from the shoots could explain this stimulation, presumably leading to a raise of the HATS activity. The increased demand is, however, likely due to two different physiological situations: an increased shoot biomass in the case of the pre-anthesis HN treatment (leading to an increased grain yield) and an N deficiency in the case of the post-anthesis LN treatment (leading to decreased grain yield and GNC). No effect was observed in the other conditions, which did not affect grain yield or GNC. This suggests a functional importance of the *BdNRT2A/B* in the responses to NO_3^- availability. The expression of *BdNRT3.2* was insensitive to the treatments (Fig. 9b).
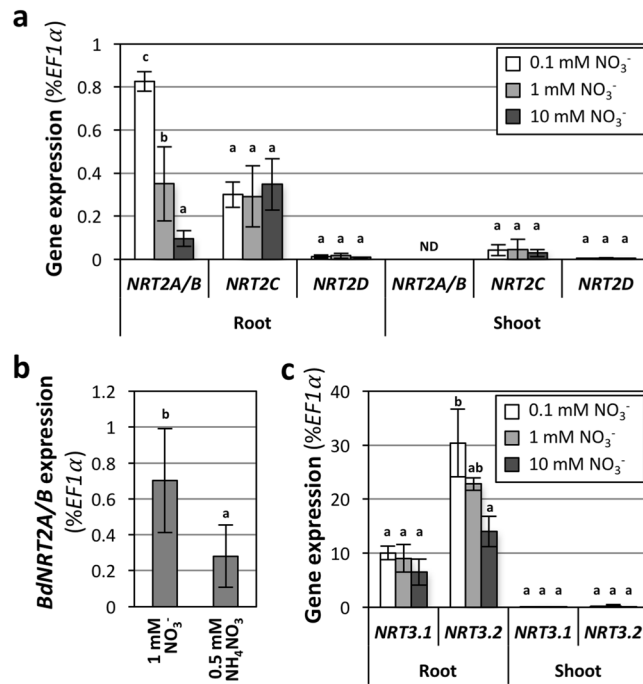
Figure 8. Response of *BdNRT2/3* expression to N availability at vegetative stage. Plants were grown in hydroponics for 17 days under the indicated N condition. **(a)** Response of *BdNRT2* genes to NO_3^- availability. *BdNRT2A* and *BdNRT2B* were quantified simultaneously due to high sequence homology. ND: not detected. **(b)** Response of *BdNRT2A/B* expression to NH_4^+. **(c)** Response of *BdNRT3* genes to NO_3^- availability. Values are normalized by *BdEF1α* expression; similar results were obtained after normalization by *BdUBC18* or *BdUbi10*. Values correspond to the mean of 4–5 biological replicates +/−SD. Letters indicate statistical groups for each gene and plant organ system (ANOVA on Log2-transformed values, p < 0.05).
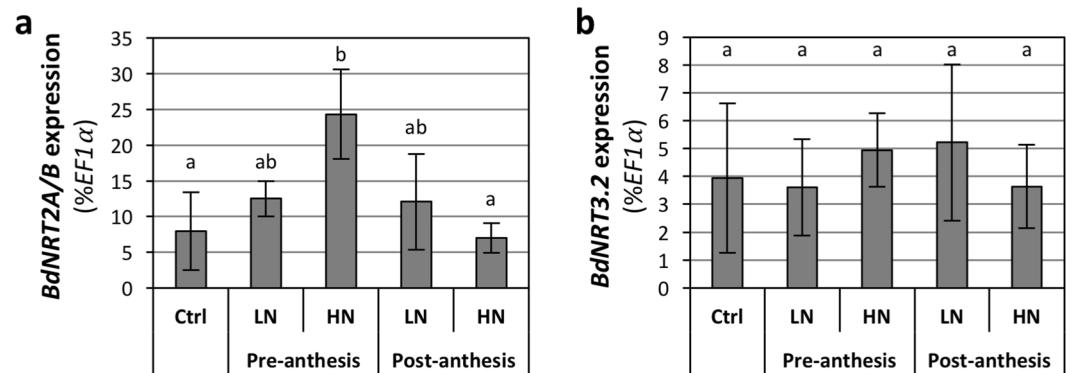
Figure 9. Effects of pre- and post-anthesis NO_3^- availability on root *BdNRT2/3* expression at reproductive stage. Growing conditions and treatments were as described in Fig. 2. LN, Ctrl and HN: 0.1, 1 and 10 mM NO_3^-, respectively. Plants were harvested 2 weeks after anthesis. **(a)** *BdNRT2A/B* expression. The genes were quantified simultaneously due to high sequence homology. **(b)** *BdNRT3.2* expression. Values are normalized by *BdEF1α* expression; similar results were obtained after normalization by *BdUBC18* or *BdUbi10*. Values correspond to the mean of 4–5 biological replicates +/−SD. Letters indicate statistical groups (ANOVA on Log2-transformed values, p < 0.05).

Conclusion

Taken together, our data indicate that the developmental and physiological responses of Brachypodium (Bd21-3 accession) to N availability are comparable to previously studied C3 temperate cereals, such as wheat and barley. Specifically, NO_3^- supply affects vegetative growth, shoot/root ratio, tiller formation, spike development, grain number per plant, grain yield and grain protein content. A high NHI, similar to what has been described in major cereals, was also observed. In addition to constitutive/inducible HATS and to a constitutive LATS, an inducible LATS was identified as a component of root NO_3^- uptake systems, as previously highlighted in wheat.

Additionally, we revealed several specificities of Brachypodium Bd21-3 that are of special interest for crop improvement. For instance, understanding the basis of the unusually high GNC (despite a low N remobilization)

in this model would be valuable towards an increased GPC in wheat. The post-anthesis NO_3^- uptake seems to furnish a large part of grain N in Brachypodium Bd21-3, even under low supply condition. This will need to be further investigated under different experimental conditions and/or on several Brachypodium accessions. The knowledge gained from this could subsequently be used to improve NUE in cereals. Similarly, the identification of the molecular origin of the high constitutive HATS in Brachypodium Bd21-3 would be instrumental in enhancing the NO_3^- uptake capacity of cereals in conditions of low availability. As a first insight, we identified *BdNRT2/3* genes potentially involved in constitutive and/or inducible HATS component.

Overall, the data identify the Bd21-3 accession of Brachypodium as a good model to decipher, at the physiological and molecular levels, the mechanisms involved in N metabolism in C3 temperate cereals. Based on our results, it will be beneficial to characterize a set of Brachypodium accessions, in order to distinguish traits that are specific to Bd21-3 from traits conserved in the entire species. Thus, our study provides the bases for candidate-gene and natural-variability approaches to identify molecular players affecting N nutrition and NUE in Brachypodium, towards the development of new cereal varieties with enhanced NUE in low N supply conditions.

Materials and Methods

Plant material and culture conditions. In this study, *Brachypodium distachyon* accession Bd21-3 was used. In the experiments, anthesis stage was defined as 7 days after emergence of the first spike[63].

Plants grown on sand were cultivated in a growth chamber under the following conditions: 8/16 h light/dark cycle, 150 μmol photons.m^{-2}.s^{-1} irradiation, 21/17 °C day/night temperature, 80% hygrometry. The basal nutrient medium contained 0.25 mM KH_2PO_4, 0.25 mM $MgSO_4$, 27 μM Na-Fe(III)-EDTA, 243 μM $(NH_4)_6Mo_7O_{24}$, 0.4 μM H_3BO_3, 118 μM $MnSO_4$, 10 μM de $CuSO_4$ and 34.8 μM $ZnSO_4$. For 0.1 mM NO_3^- solution, the medium was supplemented with 0.1 mM KNO_3, 0.35 mM K_2SO_4 and 0.25 mM $CaCl_2$. For 2 mM NO_3^- solution, the medium was supplemented with 1.75 mM KNO_3, 0.125 mM $Ca(NO_3)_2$ and 0.125 mM $CaCl_2$. For 10 mM NO_3^- solution, the medium was supplemented with 5 mM KNO_3, 2.5 mM $Ca(NO_3)_2$ and 0.2 mM NaCl. Plants were provided with nutrient solution 3 times a week in excess, and flow-through was discarded. Plants were harvested 35 days after sowing, 1 h after the start of the light period. Root system and individual tillers were weighed separately, frozen in liquid nitrogen and stored at −80 °C.

Plants grown in hydroponics were cultivated in a growth chamber under the following conditions: 18/6 h light/dark cycle, 250 μmol photons.m^{-2}.s^{-1} irradiation, 22/19 °C day/night temperature, 65/90% hygrometry day/night. Grains were stratified 3–4 days at 4 °C in water, germinated in the dark at 20 °C in water for one week, and transferred to a hydroponic system composed of 15 L opaque tanks covered with perforated opaque lids. Each tank hosted 32 young plants at the beginning of the experiment, and down to 6 plants after anthesis to avoid a rapid depletion of the nutrient solution. Solution was fully renewed 2–3 times a week, and the steadiness of NO_3^- concentration was validated using MQuant^{TM} Nitrate Test strips (Merck) and Nitrachek 404 quantification device (Quomed Ltd). Basal hydroponic solution was adapted from wheat studies[74,97] and contained 1 mM KH_2PO_4, 2 mM $MgSO_4$, 5 mM KCl, 50 μM Na-Fe(III)–EDTA, 4.5 μM $MnCl_2$, 10 μM H_3BO_3, 0.7 μM $ZnCl_2$, 0.4 μM $CuSO_4$, 0.22 μM MoO_4Na_2. N-depleted medium was supplemented with 3.25 mM $CaCl_2$. The 0.01 mM NO_3^- medium was supplemented with 0.005 mM KNO_3, 0.0025 mM $Ca(NO_3)_2$ and 3 mM $CaCl_2$. The 0.1 mM NO_3^- medium was supplemented with 0.05 mM $Ca(NO_3)_2$ and 3 mM $CaCl_2$. The 0.2 mM NO_3^- medium was supplemented with 0.1 mM KNO_3, 0.05 mM $Ca(NO_3)_2$ and 3 mM $CaCl_2$. The 1 mM NO_3^- medium was supplemented with 0.5 mM $Ca(NO_3)_2$ and 3 mM $CaCl_2$. The 2 mM NO_3^- medium was supplemented with 1 mM KNO_3, 0.5 mM $Ca(NO_3)_2$ and 3 mM $CaCl_2$. The 10 mM NO_3^- medium was supplemented with 5 mM KNO_3, 2.5 mM $Ca(NO_3)_2$ and 2 mM $CaCl_2$ and was deprived of KCl. For characterization on fresh material, plants were harvested at the middle of light period, roots were rinsed 1 min in 0.1 mM $CaSO_4$, the plant parts were weighed separately, frozen in liquid nitrogen and stored at −80 °C until analyses. For end of cycle analyses, plants were harvested after full senescence, roots were rinsed 1 min in 0.1 mM $CaSO_4$, roots, shoots and grains were collected separately and dried 48 h at 70 °C.

Measurement of ^{15}N, N and C contents and procedures for ^{15}N labeling. Total N, C and ^{15}N contents were quantified on 2–5 mg DW aliquots of ground tissues, dried at 70 °C for 48 h. The method is based on the Dumas combustion analysis which consist in a flash combustion of the samples in presence of He and O_2 at 950 °C. The C and N elements are detected by gas chromatography on a FLASH 2000 Organic Elemental Analyzer (Thermo Fisher Scientific, Villebon, France). The $^{15}N/^{14}N$ isotopic ratio is subsequently quantified by a coupled mass spectroscope (Delta V advantage IRMS; Thermo Fisher Scientific, Villebon, France).

Protocol for NO_3^- influx was adapted from Delhon and colleagues[98]. Plants grown in hydroponics were sequentially transferred to 0.1 mM $CaSO_4$ for 1 min and to the basal nutrient solution (see above) supplemented with 3 mM $CaCl_2$ and 0, 0.01, 0.025, 0.05, 0.1, 0.2, 0.5, 1, 2, 5 or 10 mM $^{15}NO_3^-$ (added as a mix of $K^{15}NO_3^-$ and $Ca(^{15}NO_3)_2$ at a molar ratio 2:1; 99% ^{15}N atom) for 5 min. The roots were washed for 1 min in 0.1 mm $CaSO_4$, shoots and roots were harvested separately, weighted and frozen in liquid nitrogen.

^{15}N labeling procedure and calculation for the estimation of post-anthesis N fluxes were performed as previously described[71]. Five days ^{15}N pulse was performed on 30 days-old plants (vegetative stage) by replacing the NO_3^- source of 0.2 mM NO_3^- medium by $^{15}NO_3^-$ (mix of $K^{15}NO_3^-$ and $Ca(^{15}NO_3)_2$ at a molar ratio 2:1; 2.5% ^{15}N atom). Roots were subsequently rinsed 1 min in 0.1 mM $CaSO_4$ and plants were transferred back to a non-labeled 0.2 mM NO_3^- medium, before being transferred to 0.01, 0.2 or 10 mM NO_3^- media at anthesis stage. Plants were harvested either at anthesis (to map the ^{15}N distribution at the end of vegetative phase) or after full senescence of the plant. Roots, shoots and spikes were collected separately, dried 48 h at 70 °C and weighted.

Measure of NO_3^- content. Nitrate content was measured by a spectrophotometric method adapted from Miranda and colleagues[99] after extraction in water of 10 mg FW or 1–2 mg DW ground tissues. The principle of this method is a reduction of nitrate by vanadium (III) through the acidic Griess reaction. The Griess reagent is a mixed solution of VCl_3 (2.5% w/v), N-1-naphtylethylenediamine (0.05% w/v) and sulfanilamide (1% w/v) in 0.5 M HCl. It was added to plant extracts in equal proportion. After 2 hours of incubation at 60 °C, the diazoniium product was measured spectrophotometrically at 540 nm.

Amino Acid and protein analyses. Free amino acids content and composition were determined after a three-step ethanol–water extraction (80%, 50% (v/v), then water at 4 °C) on 30 mg DW (for vegetative tissues) or 50 mg DW (for grains) of ground material, according to Ferrario-Méry and colleagues[100]. Free amino acid content was quantified by ninhydrin colorimetric analysis[101]. The amino acid composition was determined by ion-exchange chromatography using the AminoTac JLC-500/V amino acid analyzer according to the instructions of the manufacturer (JEOL (Europe), Croissy-sur-Seine, France).

Protein content was determined after extraction of 50 mg DW of grain powder in 0.062 M Tris-HCl pH 6.8, and 2% SDS[102]. Extractable proteins were quantified by the the RC DC™ (reducing agent and detergent compatible) protein assay kit (Bio-Rad Laboratories, Hercules, California, USA) based on the Lowry protocol. Samples of extractable proteins were separated on 10% SDS-PAGE gels and stained with Coomassie Brilliant Blue R250 (Sigma, St Louis, MO, USA).

RNA extraction and qRT-PCR. Total RNAs were isolated using Trizol® reagent (Ambion, Life Technologies), treated by DNase I (Thermo Scientific) and reverse-transcribed using oligo(dT)$_{18}$ primer and RevertAid H Minus Reverse Transcriptase (Thermo Scientific), according to the manufacturer's protocols. Reactions of qPCR were performed using LightCycler-FastStart DNA Master SYBR Green I kit (Roche) on a Realplex MasterCycler (Eppendorf), according to the manufacturer's protocol. Primer sequences are specified in Supporting Information Table S4. Primers for housekeeping genes *BdEf1α*, *BdUBC18* and *BdUbi10* were selected from previous report[103]. Primer efficiency (eff) was determined at each run using a standard curve on a pool of cDNA. Normalized expression value was calculated using the formula: Normalized Relative Quantity = $(1/\text{eff}^{Ct})_{HK}/(1/\text{eff}^{Ct})_{GOI}$, with Hk and GOI corresponding to Housekeeping gene and Gene Of Interest[104], respectively. Statistical analyses of qRT-PCR data were performed by ANOVA on log2-transformed values[104].

Statistical analyses. All statistical tests have been performed with the R software, using the *multcomp*, *coin* and *RVAideMemoire* packages[105–107]. One-way ANOVA tests (qRT-PCR data) were used in conjunction with Tukey tests for the analysis of qRT-PCR data. Non-parametric one-way ANOVAs were performed using an approximate Fisher-Pitman permutation test, followed by a pairwise comparison test with the calculation of an adjusted *P*-value (fdr method).

Data Availability

All the relevant data supporting the findings are available from the corresponding author on reasonable request.

References

1. Alexandratos, N. & Bruinsma, J. World agriculture: towards 2015/2030: an FAO perspective. *Land use policy* **20**, 375 (2012).
2. Tilman, D., Cassman, K. G., Matson, P. A., Naylor, R. & Polasky, S. Agricultural sustainability and intensive production practices. *Nature* **418**, 671–7 (2002).
3. Mann, C. C. Crop Scientists Seek a New Revolution. *Science (80-.)*. **283**, 310–316 (1999).
4. Kamprath, E. J., Moll, R. H. & Rodriguez, N. Effects of nitrogen fertilization and recurrent selection on performance of hybrid populations of corn. *Agron. J.* **74**, 955–958 (1982).
5. Cassman, K. G. Ecological intensification of cereal production systems: yield potential, soil quality, and precision agriculture. *Proc. Natl. Acad. Sci. USA* **96**, 5952–9 (1999).
6. Masclaux-Daubresse, C. *et al*. Nitrogen uptake, assimilation and remobilization in plants: challenges for sustainable and productive agriculture. *Ann. Bot.* **105**, 1141–57 (2010).
7. Chardon, F., Noël, V. & Masclaux-Daubresse, C. Exploring NUE in crops and in Arabidopsis ideotypes to improve yield and seed quality. *J. Exp. Bot.* **63**, 3401–12 (2012).
8. Sylvester-Bradley, R. & Kindred, D. R. Analysing nitrogen responses of cereals to prioritize routes to the improvement of nitrogen use efficiency. *J. Exp. Bot.* **60**, 1939–51 (2009).
9. Gojon, A. Nitrogen nutrition in plants: rapid progress and new challenges. *J. Exp. Bot.* **68**, 2457–2462 (2017).
10. Dechorgnat, J. *et al*. From the soil to the seeds: the long journey of nitrate in plants. *J. Exp. Bot.* **62**, 1349–1359 (2011).
11. Xu, G., Fan, X. & Miller, A. J. Plant nitrogen assimilation and use efficiency. *Annu. Rev. Plant Biol.* **63**, 153–82 (2012).
12. Havé, M., Marmagne, A., Chardon, F. & Masclaux-Daubresse, C. Nitrogen remobilisation during leaf senescence: lessons from Arabidopsis to crops. *J. Exp. Bot.* **68**, erw365 (2017).
13. Girin, T. *et al*. Brachypodium: a promising hub between model species and cereals. *J. Exp. Bot.* **65**, 5683–5696 (2014).
14. Dawson, J. C., Huggins, D. R. & Jones, S. S. Characterizing nitrogen use efficiency in natural and agricultural ecosystems to improve the performance of cereal crops in low-input and organic agricultural systems. *F. Crop. Res.* **107**, 89–101 (2008).
15. Marschner, H. *Mineral Nutrition of Higher Plants. Mineral Nutrition of Higher Plants*, https://doi.org/10.1016/B978-012473542-2/50004-3 (Elsevier, 1995).
16. Miller, A. J., Fan, X., Orsel, M., Smith, S. J. & Wells, D. M. Nitrate transport and signalling. *J. Exp. Bot.* **58**, 2297–2306 (2007).
17. Miller, A. J. & Cramer, M. D. Root Nitrogen Acquisition and Assimilation. *Plant Soil* **274**, 1–36 (2005).
18. Huang, N., Liu, K., Lo, H. & Tsay, Y. Cloning and Functional Characterization of an Arabidopsis Nitrate Transporter Gene That Encodes a Constitutive Component of Low-Affinity Uptake. *Plant Cell* **11**, 1381–1392 (1999).
19. Filleur, S. *et al*. An arabidopsis T-DNA mutant affected in Nrt2 genes is impaired in nitrate uptake. *FEBS Lett.* **489**, 220–4 (2001).
20. Vidmar, J. J. *et al*. Regulation of high-affinity nitrate transporter genes and high-affinity nitrate influx by nitrogen pools in roots of barley. *Plant Physiol.* **123**, 307–18 (2000).
21. Yin, L.-P., Li, P., Wen, B., Taylor, D. & Berry, J. O. Characterization and expression of a high-affinity nitrate system transporter gene (TaNRT2.1) from wheat roots, and its evolutionary relationship to other NTR2 genes. *Plant Sci.* **172**, 621–631 (2007).

22. Krapp, A. *et al*. Expression studies of Nrt2:1Np, a putative high-affinity nitrate transporter: Evidence for its role in nitrate uptake. *Plant J*. **14**, 723–731 (1998).

23. Kiba, T. & Krapp, A. Plant nitrogen acquisition under low availability: Regulation of uptake and root architecture. *Plant Cell Physiol*. **57**, 707–714 (2016).

24. Vidmar, J. J., Zhuo, D., Siddiqi, M. Y. & Glass, A. D. M. Isolation and Characterization of HvNRT2.3 and HvNRT2.4, cDNAs Encoding High-Affinity Nitrate Transporters from Roots of Barley. *Plant Physiol*. **122**, 783–792 (2000).

25. Glass, A. D. M. *et al*. Nitrogen transport in plants, with an emphasis on the regulation of fluxes to match plant demand §. **1**, 199–207 (2001).

26. Crawford, N. M. & Glass, A. D. M. Molecular and physiological aspects of nitrate uptake in plants. *Trends Plant Sci*. **3**, 389–395 (1998).

27. Girin, T. *et al*. Identification of a 150 bp cis-acting element of the AtNRT2.1 promoter involved in the regulation of gene expression by the N and C status of the plant. *Plant. Cell Environ*. **30**, 1366–80 (2007).

28. Orsel, M. *et al*. Characterization of a two-component high-affinity nitrate uptake system in Arabidopsis. Physiology and protein-protein interaction. *Plant Physiol*. **142**, 1304–17 (2006).

29. Plett, D. *et al*. Dichotomy in the NRT Gene Families of Dicots and Grass Species. *PLoS One* **5**, e15289 (2010).

30. Morot-Gaudry, J.-F. *Nitrogen assimilation by plants - Physiological, biochemical and molecular espects*. (CRC Press, 2001).

31. Masclaux, C., Quilleré, I., Gallais, A. & Hirel, B. The challenge of remobilisation in plant nitrogen economy. A survey of physio agronomic and molecular approaches. *Ann. Appl*. 69–81 (2001).

32. Van Sanford, D. A. & Mackown, C. T. Cultivar Differences in Nitrogen Remobilization During Grain Fill in Soft Red Winter Wheat. *Crop Sci*. **300**, 295–300 (1987).

33. Przulj, N. & Momčilović, V. Dry matter and nitrogen accumulation and use in spring barley. **2003**, 36–47 (2003).

34. Gregersen, P. L., Culetic, A., Boschian, L. & Krupinska, K. Plant senescence and crop productivity. *Plant Mol. Biol*. **82**, 603–22 (2013).

35. Brevis, J. C. & Dubcovsky, J. Effects of the Chromosome Region Including the Locus on Wheat Grain and Protein Yield. *Crop Sci*. **50**, 93 (2010).

36. Uauy, C., Distelfeld, A., Fahima, T., Blechl, A. & Dubcovsky, J. A NAC Gene regulating senescence improves grain protein, zinc, and iron content in wheat. *Science (80-.)*. **314**, 1298–301 (2006).

37. Bogard, M. *et al*. Deviation from the grain protein concentration-grain yield negative relationship is highly correlated to post-anthesis N uptake in winter wheat. *J. Exp. Bot*. **61**, 4303–12 (2010).

38. Monaghan, J. M., Snape, J. W., Chojecki, A. J. S. & Kettlewell, P. S. The use of grain protein deviation for identifying wheat cultivars with high grain protein concentration and yield. *Euphytica* **122**, 309–317 (2001).

39. Ingram, P. A. *et al*. High-throughput imaging and analysis of root system architecture in *Brachypodium distachyon* under differential nutrient availability. *Philos. Trans. R. Soc. Lond. B. Biol. Sci*. **367**, 1559–69 (2012).

40. Poiré, R. *et al*. Digital imaging approaches for phenotyping whole plant nitrogen and phosphorus response in *Brachypodium distachyon*. *J. Integr. Plant Biol*. **56**, 781–796 (2014).

41. Hong, J. J. *et al*. Diversity of morphology and function in arbuscular mycorrhizal symbioses in *Brachypodium distachyon*. *Planta* **236**, 851–65 (2012).

42. Lawlor, D. W., Lemaire, G. & Gastal, F. In *Plant Nitrogen* (eds Lea, P. J. & Morot-Gaudry, J.-F.) 343–367, https://doi.org/10.1007/978-3-662-04064-5_13 (Springer Berlin Heidelberg, 2001).

43. Brouwer, R. Nutritive influences on the distribution of dry matter in the plant. *Netherl. J. Agric. Sci*. **10**, 361–376 (1962).

44. Oscarson, P. The strategy of the wheat plant in acclimating growth and grain production to nitrogen availability. *J. Exp. Bot*. **51**, 1921–1929 (2000).

45. Dupont, F. M. & Altenbach, S. B. Molecular and biochemical impacts of environmental factors on wheat grain development and protein synthesis. *J. Cereal Sci*. **38**, 133–146 (2003).

46. Beatty, P. H. *et al*. Nitrogen use efficiencies of spring barley grown under varying nitrogen conditions in the field and growth chamber. *Ann. Bot*. **105**, 1171–82 (2010).

47. Garcia del Moral, L., Ramos, J. & Recalde, L. Relationships between vegetative growth, grain yield and grain protein content in six winter barley cultivars. *Can. J. plant Sci*. **532**, 523–532 (1985).

48. Kichey, T., Hirel, B., Heumez, E., Dubois, F. & Le Gouis, J. In winter wheat (Triticum aestivum L.), post-anthesis nitrogen uptake and remobilisation to the grain correlates with agronomic traits and nitrogen physiological markers. *F. Crop. Res*. **102**, 22–32 (2007).

49. Taulemesse, F., Gouis, J. L., Gouache, D., Gibon, Y. & Allard, V. Bread wheat (Triticum aestivum L.) grain protein concentration is related to early post-flowering nitrate uptake under putative control of plant satiety level. *PLoS One* **11**, 1–21 (2016).

50. Gastal, F. & Lemaire, G. N uptake and distribution in crops: an agronomical and ecophysiological perspective. *J. Exp. Bot*. **53**, 789–799 (2002).

51. Justes, E., Mary, B., Meynard, J.-M., Machet, J.-M. & Thelier-Huche, L. Determination of a Critical Nitrogen Dilution Curve for Winter Wheat Crops. *Ann. Bot*. **74**, 397–407 (1994).

52. Makino, A. Photosynthesis, grain yield, and nitrogen utilization in rice and wheat. *Plant Physiol*. **155**, 125–9 (2011).

53. Jamieson, P. D., Martin, R. J. & Francis, G. S. Drought influences on grain yield of barley, wheat, and maize. *New Zeal. J. Crop. Hortic. Sci*. **23**, 55–66 (1995).

54. Fischer, R. A., Aguilar, I. & Laing, D. R. Post-anthesis sink size in a high-yielding dwarf wheat: Yield response to grain number. *Aust. J. Agric. Res*. **28**, 165–175 (1977).

55. Maidl, F., Sticksel, E., Retzer, F. & Frschbeck, G. Effect of Varied N-fertilization on Yield Formation of Winter Wheat under Particular Consideration of Mainstems and Tillers. *J. Agron. Crop Sci*. **180**, 15–22 (1998).

56. Derkx, A. P., Orford, S., Griffiths, S., Foulkes, M. J. & Hawkesford, M. J. Identification of differentially senescing mutants of wheat and impacts on yield, biomass and nitrogen partitioning. *J. Integr. Plant Biol*. **54**, 555–66 (2012).

57. Cai, S. *et al*. Grain protein content variation and its association analysis in barley. *BMC Plant Biol*. **13**, 35 (2013).

58. Gali, V. J & Brown, C. G. Assisting decision-making in Queensland barley production through chance constrained programming. *Aust. J. Agric. Resour. Econ*. **44**, 269–287 (2000).

59. Branlard, G. & Dardevet, M. Diversity of grain proteins and bread wheat quality: I. Correlation between Gliadin Bands and Flour quality characteristics. *J. Cereal Sci*. **3**, 329–343 (1985).

60. Xu, Y. *et al*. Mapping QTLs for yield and nitrogen-related traits in wheat: influence of nitrogen and phosphorus fertilization on QTL expression. *Theor. Appl. Genet*. **127**, 59–72 (2014).

61. Barraclough, P. B. *et al*. Nitrogen efficiency of wheat: Genotypic and environmental variation and prospects for improvement. *Eur. J. Agron*. **33**, 1–11 (2010).

62. Sosulski, F. W. & Imafidon, G. I. Amino acid composition and nitrogen-to-protein conversion factors for animal and plant foods. *J. Agric. Food Chem*. **38**, 1351–1356 (1990).

63. Guillon, F. *et al*. A comprehensive overview of grain development in *Brachypodium distachyon* variety Bd21. *J. Exp. Bot*. **63**, 739–55 (2012).

64. Larré, C. *et al*. *Brachypodium distachyon* grain: identification and subcellular localization of storage proteins. *J. Exp. Bot*. **61**, 1771–83 (2010).

65. Martre, P., Porter, J. R., Jamieson, P. D. & Triboï, E. Modeling grain nitrogen accumulation and protein composition to understand the sink/source regulations of nitrogen remobilization for wheat. *Plant Physiol.* **133**, 1959–67 (2003).

66. Wuest, S. B. & Cassman, K. G. Fertilizer-Nitrogen Use Efficiency of Irrigated Wheat: I. Uptake Efficiency of Preplant versus Late-Season Application. *Agron. J.* **84**, 682–688 (1992).

67. Shewry, P. R. Improving the protein content and composition of cereal grain. *J. Cereal Sci.* **46**, 239–250 (2007).

68. Shewry, P. R., Tatham, A. S. & Halford, N. G. Nutritional control of storage protein synthesis in developing grain of wheat and barley. *Plant Growth Regul.* **34**, 105–111 (2001).

69. Altenbach, S. B. *et al*. Differential effects of a post-anthesis fertilizer regimen on the wheat flour proteome determined by quantitative 2-DE. *Proteome Sci.* **9**, 1–13 (2011).

70. Žilić, S., Barać, M., Pešić, M., Dodig, D. & Ignjatović-Micić, D. Characterization of proteins from grain of different bread and durum wheat genotypes. *Int. J. Mol. Sci.* **12**, 5878–5894 (2011).

71. Salon, C. *et al*. In *Plant Metabolic Networks: Methods and Protocols*. 1090, 335–346 (2014).

72. Ta, C. T. & Weiland, R. T. Nitrogen Partitioning in Maize during Ear Development. *Crop Sci.* **32**, 443 (1992).

73. Triboi, E. & Triboi-Blondel, A. M. Productivity and grain or seed composition: A new approach to an old problem. *Eur. J. Agron.* **16**, 163–186 (2002).

74. Taulemesse, F., Le Gouis, J., Gouache, D., Gibon, Y. & Allard, V. Post-Flowering Nitrate Uptake in Wheat Is Controlled by N Status at Flowering, with a Putative Major Role of Root Nitrate Transporter NRT2.1. *PLoS One* **10**, e0120291 (2015).

75. Worland, B., Robinson, N., Jordan, D., Schmidt, S. & Godwin, I. Post-anthesis nitrate uptake is critical to yield and grain protein content in Sorghum bicolor. *J. Plant Physiol.* **216**, 118–124 (2017).

76. Borrell, A. K. & Hammer, G. L. Nitrogen dynamics and the physiological basis of stay-green in Sorghum. *Crop Sci.* **40**, 1295–1307 (2000).

77. Rajcan, I. & Tollenaar, M. Source:sink ratio and leaf senescence in maize: I. Dry matter accumulation and partitioning during grain filling. *F. Crop. Res.* **60**, 245–253 (1999).

78. Barneix, A. J. Physiology and biochemistry of source-regulated protein accumulation in the wheat grain. *J. Plant Physiol.* **164**, 581–90 (2007).

79. Gooding, M. J., Gregory, P. J., Ford, K. E. & Ruske, R. E. Recovery of nitrogen from different sources following applications to winter wheat at and after anthesis. *F. Crop. Res.* **100**, 143–154 (2007).

80. Papakosta, D. K. & Gagianas, a. a. Nitrogen and Dry Matter Accumulation, Remobilization, and Losses for Mediterranean Wheat during Grain Filling. *Agron. J.* **83**, 864 (1991).

81. Bancal, P. Decorrelating source and sink determinism of nitrogen remobilization during grain filling in wheat. *Ann. Bot.* **103**, 1315–24 (2009).

82. Schjoerring, J. K., Bock, J. G. H., Gammelvind, L., Jensen, C. R. & Mogensen, V. O. Nitrogen incorporation and remobilization in different shoot components of field-grown winter oilseed rape (Brassica napus L.) as affected by rate of nitrogen application and irrigation. *Plant Soil* **177**, 255–264 (1995).

83. Siddiqi, M. Y., Glass, A. D. M., Ruth, T. J. & Rufty, T. W. Studies of the Uptake of Nitrate in Barley I. Kinetics of 13NO3- Influx. **93**, 1426–1432 (1990).

84. Siddiqi, M. Y., Glass, A. D. M., Ruth, T. J. & Fernando, M. Studies of the Regulation of Nitrate Influx by Barley Seedlings Using $13NO_3^-$. *Plant Physiol.* 806–813 (1989).

85. Cai, C. *et al*. Regulation of the high-affinity nitrate transport system in wheat roots by exogenous abscisic acid and glutamine. *J. Integr. Plant Biol.* **49**, 1719–1725 (2007).

86. Le Deunff, E. & Malagoli, P. An updated model for nitrate uptake modelling in plants. I. Functional component: cross-combination of flow–force interpretation of nitrate uptake isotherms, and environmental and in planta regulation of nitrate influx. *Ann. Bot.* **113**, 991–1005 (2014).

87. Forde, B. & Clarkson, D. Nitrate and Ammonium Nutrition of Plants: Physiological and Molecular Perspectives. *Adv. Bot. Res.*, https://doi.org/10.1016/S0065-2296(08)60226-8 (1999).

88. Kalinata, P. & Nair, T. V. Variability In Kinetics Of Nitrate Uptake In Wheat Genotypes. *Indian J. Plant Physiol.* **6**, 411–413 (2001).

89. Trčkova, M., Stehno, Z. & Raimanová, I. Nitrate uptake and N allocation in Triticum aestivum L. and Triticum durum Desf. seedlings. *Plant Soil Environ.* **52**, 88–96 (2006).

90. Das, R., Jain, V., Aravind, S., Barman, M. & Srivastava, G. C. Kinetics Of Nitrate Uptake System In Wheat Genotypes. *Indian J. Plant Physiol.* **11**, 160–165 (2006).

91. He, M. *et al*. Leaf nitrogen and phosphorus of temperate desert plants in response to climate and soil nutrient availability. *Sci. Rep.* **4**, 6932 (2014).

92. Vogel, J. P. & Hill, T. High-efficiency Agrobacterium-mediated transformation of *Brachypodium distachyon* inbred line Bd21-3. *Plant Cell Rep.* **27**, 471–8 (2008).

93. Glass, A. D. M., Shaff, J. E. & Kochian, L. V. Studies of the Uptake of Nitrate in Barley IV. Electrophysiology. 456–463 (1992).

94. Pang, J., Milroy, S. P., Rebetzke, G. J. & Palta, J. A. The influence of shoot and root size on nitrogen uptake in wheat is affected by nitrate affinity in the roots during early growth. *Funct. Plant Biol.* **42**, 1179–1189 (2015).

95. Min, X., Siddiqi, M. Y., Guy, R. D., Glass, A. D. M. & Kronzucker, H. J. A comparative kinetic analysis of nitrate and ammonium influx in two early-successional tree species of temperate and boreal forest ecosystems. *Plant, Cell Environ.* **23**, 321–328 (2000).

96. Feng, H. *et al*. Spatial expression and regulation of rice high-affinity nitrate transporters by nitrogen and carbon status. *J. Exp. Bot.* **62**, 2319–2332 (2011).

97. Castle, S. & Randall, P. Effects of Sulfur Deficiency on the Synthesis and Accumulation of Proteins in the Developing Wheat Seed. *Aust. J. Plant Physiol.* **14**, 503 (1987).

98. Delhon, P., Gojon, A., Tillard, P. & Passama, L. Diurnal regulation of N03 uptake in soybean plants I. Changes in N03 influx, efflux, and N utilization in the plant during the day/night cycle. *J. Exp. Bot.* **46**, 1585–1594 (1995).

99. Miranda, K. M., Espey, M. G. & Wink, D. A. A Rapid, Simple Spectrophotometric Method for Simultaneous Detection of Nitrate and Nitrite. *Nitric Oxide* **5**, 62–71 (2001).

100. Ferrario-Méry, S. *et al*. Physiological characterisation of Arabidopsis mutants affected in the expression of the putative regulatory protein PII. *Planta* **223**, 28–39 (2005).

101. Rosen, H. A modified ninhydrin colorimetric analysis for amino acids. *Arch. Biochem. Biophys.* **67**, 10–15 (1957).

102. Guillon, F. *et al. Brachypodium distachyon* grain: characterization of endosperm cell walls. *J. Exp. Bot.* **62**, 1001–15 (2011).

103. Hong, S.-Y., Seo, P. J., Yang, M.-S., Xiang, F. & Park, C.-M. Exploring valid reference genes for gene expression studies in *Brachypodium distachyon* by real-time PCR. *BMC Plant Biol.* **8**, 112 (2008).

104. Rieu, I. & Powers, S. J. Real-Time Quantitative RT-PCR: Design, Calculations, and Statistics. *Plant Cell Online* **21**, 1031–1033 (2009).

105. Hothorn, T., Hornik, K., van de Wiel, M. A. & Zeileis, A. Implementing a Class of Permutation Tests: The coin Package. *J. Stat. Softw. Novemb.* **28**, 2–23 (2008).

106. Bretz, F., Hothorn, T. & Westfall, P. In *Multiple Comparisons Using R* 202, https://doi.org/10.1201/9781420010909-f (Chapman and Hall/CRC, 2011).

107. Hervé, M. RVAideMemoire: Testing and Plotting Procedures for Biostatistics. Available at, https://cran.r-project.org/package=RVAideMemoire (2017).

Acknowledgements

Author Contributions

L.C.D., T.G., F.D.V., A.K. and S.F.M. conceived the experiments. L.C.D., T.G., E.F., E.P., A.M., S.C., P.B. and S.F.M. conducted the experiments. L.C.D., T.G. and S.F.M. analyzed the results. T.G. and S.F.M. wrote the manuscript. All authors reviewed the manuscript.

Additional Information

Supplementary information accompanies this paper at https://doi.org/10.1038/s41598-019-40569-8.

Competing Interests: The authors declare no competing interests.

Publisher's note: Springer Nature remains neutral with regard to jurisdictional claims in published maps and institutional affiliations.